ISBN: 978-628-95207-4-3. ISSN: 2414-6390. Digital Object Identifier: https://dx.doi.org/10.18687/LACCEI2023.1.1.806

Design of a prototype fixed-wing drone for blood packet delivery applications

Carlos Espinoza, Mechatronic Engineer[1], Jorge Villasante, Mechatronic Engineer[2], and Leonardo Vinces, Electronic Engineer[3]
[1,2,3]Universidad Peruana de Ciencias Aplicadas, Perú, u201621874@upc.edu.pe, u201621028@upc.edu.pe, leonardo.vinces@upc.pe

Abstract*– This paper proposes a fixed-wing drone design for blood packages delivery applications to solve the slow and inefficient transport system of blood units for transfusions in emergency operations in regions surrounding Lima, Peru. What is sought in this project is the structural stability of a drone to carry a maximum load of 5 kg, which will deliver parcels through an autonomously operated drop-down cabin-box. The design consists of a series of sequential steps. First, the design of the wing assembly, which mainly involves the definition of the wing profiles; analysis of the forces and moments of the schematic composition of a fixed-wing drone; and location/measurements of the drone's wing and tail. Second, the de-sign of the fuselage and cockpit-deployable box maintaining the location/measurements of the wing configuration. Finally, the static-dynamic structural analysis to evaluate the state of stress of the drone structures subjected to constant forces in the flight time. This evaluation looks for a configuration in which all the loads and forces of the mechanism are balanced.

Keywords-- Drone, Fixed wings, Structural analysis, Delivery, CFD.

I. Introduction

The lack of blood units in the country is a constant problem, thousands of people die annually due to lack of access to blood units for transfusion [2]. Added to this, the culture of blood donation in the inhabitants is little or null; Most of the people who donate do so compulsorily, because someone they know requires units [1]. That is why we see ourselves in the need to have an efficient distribution system that allows us to beat the underlying problem and deliver units upon request.

Due to this, in recent years various solutions have been designed to attack this problem of global interest, especially for developing countries.

Zipline [3], an American start-up founded in 2014, noticed that there were similar problems in Rwanda and decided to make a fixed-wing drone delivery system between one of the collection centers and the hospitals where the medical units are destined; the package in that case is released by opening a gate in the fuselage that contains it.

On the other hand, in 2018, Stanislaw Bobela [4] presented a thesis on the development of a blood delivery system in India, with the difference that in this case the drones would be of the quadcopter type powered by four electric motors and having to the fastened package, not contained.

Digital Object Identifier: (only for full papers, inserted by LACCEI).
ISSN, ISBN: (to be inserted by LACCEI).
DO NOT REMOVE

Finally, in 2019, Geoffrey Ling and Nicole Draghic [5] presented an investigation of the use of drones in the delivery of medical packages, performing a cost/time analysis and concluding that drones allow for improved response times and reduced delivery costs. transportation.

Considering the observations raised by the research shown, what is proposed in this document is a delivery system for blood packages by means of a fixed-wing drone with a drop-down container box.

The design of a preliminary prototype of a transport drone using wings and tail with properly selected airfoil profiles, and a solid structure designed, will allow achieving the necessary stability and speed to transport an expected load through force and deformation analysis.

II. Description of the Proposed Method

The main objective of this document is to design a delivery drone and analyze in detail the structure so that it can fly at the required speed and support the expected load. The proposed method is described below.

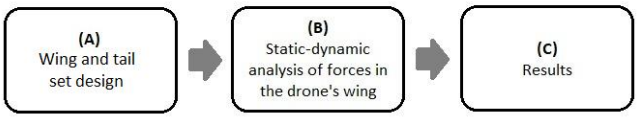

Fig. 1. Block diagram of the method.

To do this, in the first place (A), the design of the wing assembly will be carried out, that is, mainly the shape, dimensions and angles in which both the wing and the tail are arranged with respect to the fuselage, once the wing profiles have already been chosen, in order for the set to present self-stability. The complete shape of the fuselage is not of primary interest because it does not affect this first analysis; however, the frontal area and the width of the profile are of importance to be able to perform calculations.

Secondly (B), a static-dynamic analysis of the forces that influence the different components of the drone will be conducted to ensure that it can withstand the flight conditions. For this, two factors will be analyzed: (i) the lift that is distributed along the wing and its reactions, as well as the thrust that pulls from the front and the drag that pulls back; (ii) air currents impacting the wing at the speed of flight. As for the rest of the structure, it is not included in this document

because it does not have the same space restrictions and therefore it can have greater reinforcements to support the payload of up to 5kg.

A. Design of the wing and tail assembly

The choice of the wing profile represents an important decision that directly affects the design and characteristics of the drone, specifically the lift generated by the wings, but also the vertical and horizontal stabilizers located in the tail (T-shaped).

Among many profile standards the 4-digit family of the National Advisory Committee for Aeronautics (NACA) wing profile standard is used since it was the first series to be defined, being the best known and applied in different simulation software.

It is considered as NACA profile, those wing profiles that follow a standard and a specific nomenclature, which defines the geometric concept of the wing profile [6].

As shown in Fig. 2, two NACA profiles were chosen for the wing: 3412 and 4412. Because they have a similar behavior, except that the profile 4412 maintains stability at certain angles of attack slightly above the profile 3412. By placing a more stable profile at the ends, an anticipation of those angles of attack that can lead to instability without necessarily entering it is ensured in the aircraft.

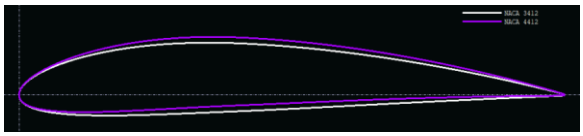

Fig. 2. NACA 3412 (white) and 4412 (purple) wing profiles.

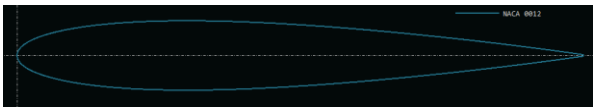

Fig. 3. NACA 0012 wing profile.

Likewise, for the tail (stabilizers and rudder) a NACA 0012 profile was chosen, because symmetry is required; that is, it does not provide a bias for any of its sides (unlike the wing that is required to provide a bias for support), and this profile has good characteristics compared to other symmetrical profiles.

With the XLFR5 software, it can be obtained the behavior of the profiles regarding the lift coefficient (Cl), the drag coefficient (Cd) and the angle of attack (AoA) as shown below:

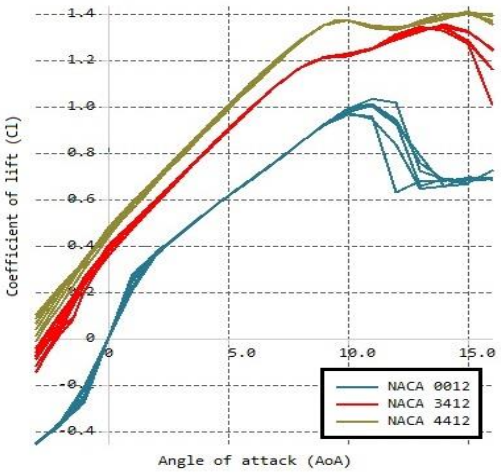

Fig. 4. Coefficient of lift vs Angle of attack.

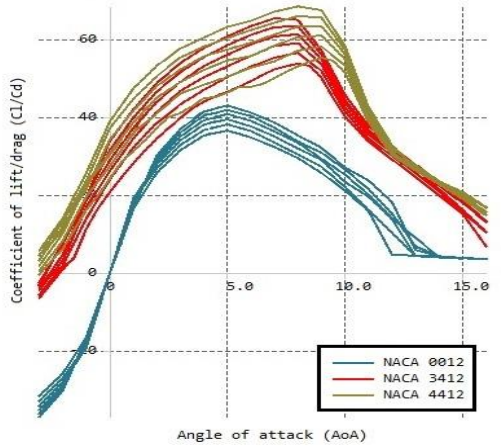

Fig. 5. Lift coefficient to drag coefficient ratio vs Angle of attack.

The 3412 and 4412 profiles have higher lift than the 0012 profile, because both are located at the wing while the third one is located at the tail. The lift to drag ratio has good lift behavior approximately between 3° to 10° of attack angles. So, considering a non-excessive angle with a good lift, an angle of attack (AoA) of 4° with a coefficient of lift (Cl) of 0.85 are defined as design parameters for this project.

With the wing profiles defined, the design needs to ensure that it has good behavior at the required speed and that it provides adequate support to be able to counteract the weight of the load. Therefore, in Fig. 6 an analysis of the forces and moments that schematically compose a fixed-wing drone is conducted.

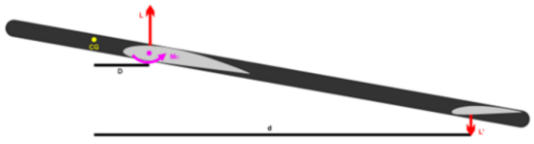

Fig. 6. Analysis of forces and moments of a fixed-wing drone

With this, it is defined that the moment generated by the tail must be contrary to the wing, since it is necessary that they are counteracted to maintain stability in the system. Therefore, the resulting moment would be as follows:

$$M = L_0 \times d - L \times D - M_0 \quad (1)$$

Expanding and simplifying, one obtains in equation (2) a representation in coefficients of moments.

$$C_m = \left((d \times S')/(S \times \underline{c})\right) \times C_L' - D \times C_L - C_{m0} \quad (2)$$

Where C_m, C_{m0} are pitch and initial position wing moment coefficients; C_L, C_L' are wing and tail lift coefficients; S, S' are wing and tail areas; D, d are distances from the center of gravity to the aerodynamic center of the wing and tail; and $\underline{c}$ is the rope of the wing profile.

The equation (2) serves to identify which parameters must be modified in the design to achieve stability. For modifications, it is important that they meet the following requirements: 10kg of lift (including payload), 100km/h of cruising speed. In this way, the minimum area of the wings can be calculated with equation (3)

$$L = (1/2) \times \rho \times S \times C_L \times V^2 \quad (3)$$

Where L is the lift [N]; ρ air density [kg/m3]; S the wing area [m2]; C_L the lift coefficient; V the velocity [m/s]. Replacing with the already obtained values, S would have to be greater or equal to 23m^2.

In that sense, with the XLFR5 software, an analysis of the coefficient of moment (C_m) is carried out with the angle of attack (AoA) since the behavior that the aircraft will have in the face of a disturbance at cruising speed of 30m/s can be determined.

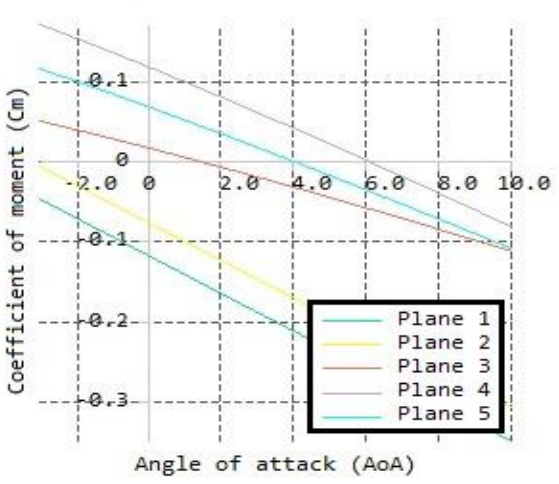

Fig. 7. Pitching moment analysis at 30m/s

Different iterations of configurations can be observed in the image, by modifying the variables mentioned in equation (2) to obtain the ideal configuration for self-stability. So, as defined an angle of attack of 4° in Fig. 4 and 5, option 5 (cyan line) is chosen. In such way, the wing configuration is as follows:

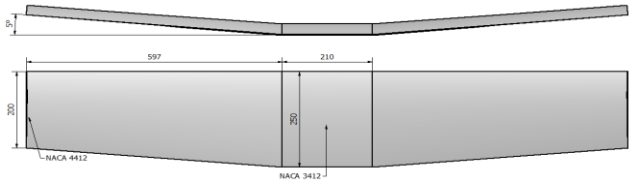

Fig. 8. Wing dimensions

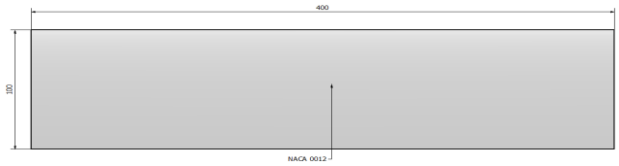

Fig. 9. Elevator dimensions

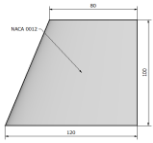

Fig. 10. Rudder dimensions

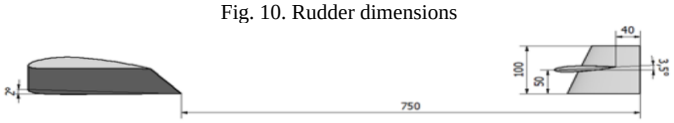

Fig. 11. Wing and tail configuration

To carry out the structural design of the fixed wing drone it is necessary to know all the measures for implementation. For this, the Autodesk Inventor software is available where the final design of the drone is made. It is also important to define an adequate structure, since this affects the resistance and performance of the drone, as well as the payload that it will be able to carry, where greater weight less load and vice versa.

This study will focus on the structure of the wing. It is planned to be used as materials for the drone, wood, and polystyrene as body-filler. With Autodesk Inventor software, it is created the next structure:

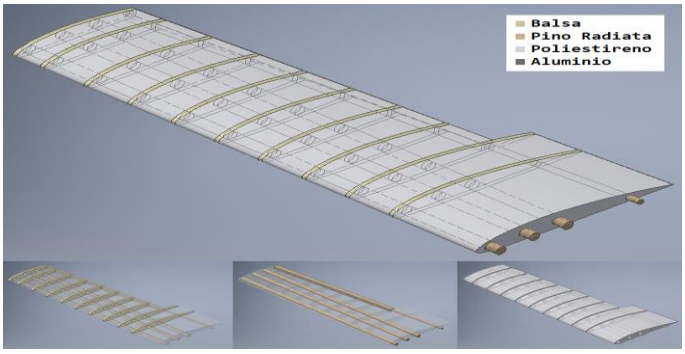

Fig. 12. Structural design of the wing drone

This section of the wing is the one that mainly exerts the lift, so it must be resistant. Added 10 balsa wooden ribs that are joined through 3 rods and 1/2 rod of radiata pine wood with the same diameters of the central wing. In the part of the 1/2 rod is coupled to a rectangular rod of the same material, which serves as a union with the wing ailerons, this union will be made with small acrylic hinges.

In section B, a stress analysis is carried out to determine the stress and deformations that can be generated in the structures. In addition, the entire drone prototype is designed as follows:

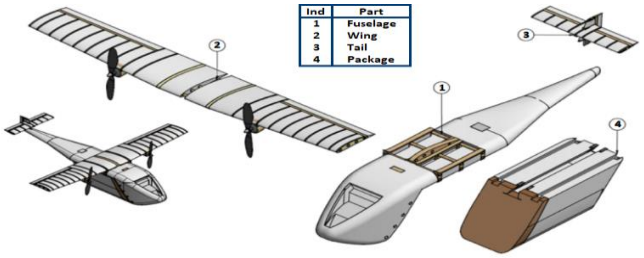

Fig. 13. Final prototype of the drone

B. Static-dynamic analysis of wing forces

In this case, it is important to evaluate the behavior of the wing because it supports the greatest interaction of forces: (i) the lift is non-homogenously distributed along the wing; (ii) the weight component of the drone is located at the internal ends, attached to the fuselage (iii) in the front of the wing, approximately in the intermediate sections on each side, the engines are found, there are located the thrust forces and at the same time the weight of each engine; (iv) the drag generated on the wing due to the lift (induced) added to the parasitic drag that we will not calculate in detail but we will choose an approximate value.

The support required to lift a drone of 10kg is approximately 100N and the weight will be the same but in the opposite direction. However, it must be considered that even though a fixed maximum load is thought, at times the support force will be superior, for example at the time of ascent and especially in the warping turns, as shown in Fig. 14.

WARPING DEGREES	0	15%	20%	30%	40%	45%	60%	75%	80%
LOAD FACTOR	1	1.03	1.06	1.15	1.31	1.41	2	3.86	5.76
LOSS SPEED-Vm	Vs	1.01	1.03	1.07	1.14	1.19	1.41	1.96	2.40
% LOSS SPEED INCREASE	0%	1%	3%	7%	14%	19%	41%	96%	140%
INDUCED RESISTANCE	Di	1.07	1.16	1.33	1.50	2	4	14.93	18.57

Fig. 14. Table load and resistance factor to different degrees of warping

Then, considering the values obtained above and the load factor shown in Fig. 14, a force value for 250N tests is determined. With that, an iterative process is carried out, where parts of the wing are reinforced with solid structures, in contrast to the rest that will have an expanded polystyrene filling.

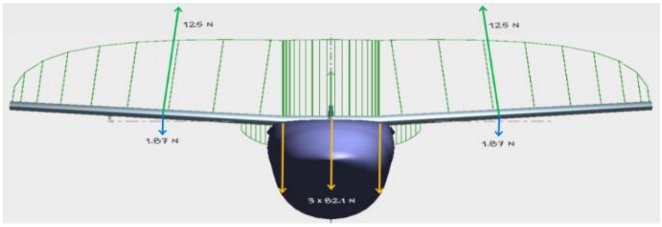

Fig. 15. Force distribution graph on the wing

$$L_d(x) = \sqrt[3]{1-(2x/0.702)^2} \quad (4)$$

As mentioned above, the lift is not a punctual force, but is distributed along the wing, represented with green arrows in Fig. 15 and follows an approximate behavior to equation (4). In addition, we have the force of weight and thrust, which are punctual forces and concentrated in the union with the fuselage (parasitic drag forces also affect here, but they are insignificant compared to the weight) and in the fastenings of each engine, respectively. The latter is found approximately at the centroid of the graph describing the distribution of forces approximately 258.6 mm from the root of the wing root according to equation (5).

$$\bar{x} = \left(\int_{x_{min}}^{x_{max}} dA \times x\right)/A \quad (5)$$

Where dA is $L_d(x)$ by dx and A is the area below the described curve.

Below are the following graphs: Fig. 16 of shear forces on the wing $V(N)$; Fig. 17 of flexing moments on the wing. Both graphs are also described in equations (6) and (7), L being the lift that gives each side of the wing, in this case 125, and M_w the weight of the engine, in this case 1.78N.

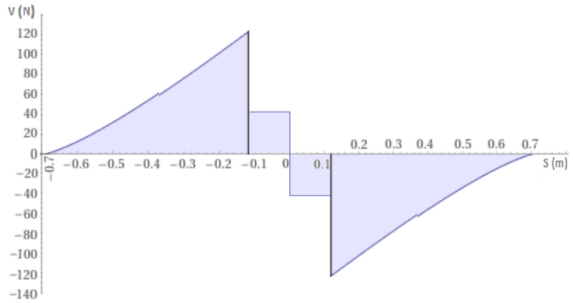

Fig. 16. Graph of shear forces by distance from the center of the wing

$$V(m) = \begin{cases} \int L_D(x)dx, & -0.702 \le x < -0.12 \\ (L - M_w)/3, & -0.12 \le x < 0 \\ (M_w - L)/3, & 0 \le x < 0.12 \\ \int L_D(x)dx, & 0.12 \le x < 0.702 \end{cases} \quad (6)$$

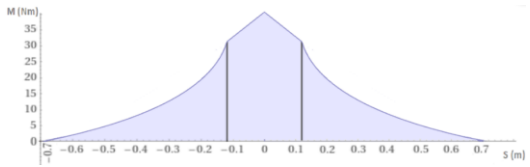

Fig. 17. Graph of bending moments by distance from the center

$$M(m) = \int V(m) \quad (7)$$

As can be seen in both images, the critical points are the joints between the wing and the fuselage located at the ends and center of the fuselage, in all these there are cutting forces of great magnitude. However, the most critical part is to the center, which also supports the maximum flexing moment with about 37Nm, so it must have the greatest reinforcement.

On the other hand, paying attention to the wing itself, in Fig. 18 the aforementioned forces do generate a certain deformation in the wing, tolerable but considerable, especially taking into account that it implies forces of great magnitude.

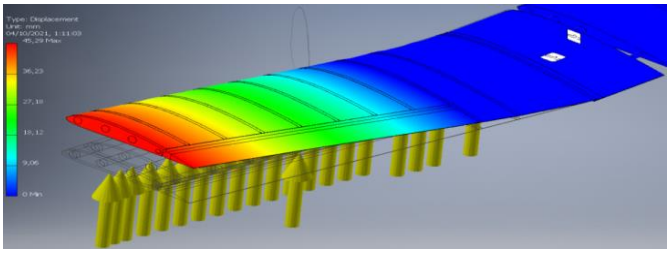

Fig. 18. Wing Stress Test in Inventor

In the same way, the approximate value of the drag must be determined in order to determine the thrust that opposes it and must be higher, to generate the accelerated movement.

To determine the drag (D), we have a formula like the lift:

$$D = (1/2) \times \rho \times S \times C_D \times V^2 \quad (8)$$

Where ρ is the density of the air [kg/m3]; S the wing surface [m2]; C_D the drag coefficient; V speed [m/s]. Replacing with the obtained values, the result would be that D is 6.4152N. To this value is added the parasitic resistance and the vortex resistance. But being negligible values compared to the support values, they will not be considered to perform a structural analysis.

Simulations are also carried out to identify deformations and stress of the wing in a wind column at a speed of approximately 30 m/s. The Von Mises criterion is used to identify stress points that may generate deformation of the distortion system. The Von Mises tension can be calculated by the expression:

$$\sigma_{VM} = \sqrt{((\sigma_1 - \sigma_2)^2 + (\sigma_2 - \sigma_3)^2 + (\sigma_1 - \sigma_3)^2)/2} \quad (9)$$

Where σ_1, σ_2 y σ_3 are main tensions. With the Ansys software, the following simulations are obtained:

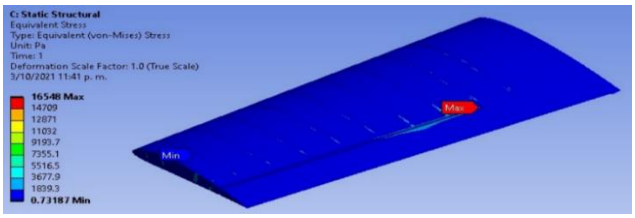

Fig. 19. Wing stress analysis in Ansys

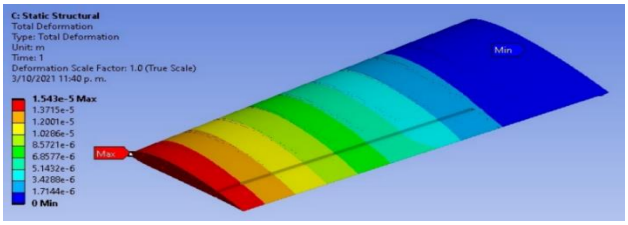

Fig. 20. Wing deformation analysis in Ansys

As can be seen in the images shown, due to the wind column generated, the wing is mostly unaffected: its deformation is negligible, compared to the dimensions of the structure and the stress it supports in general has very low values. Although in the latter case, it is appreciated that the joints have the greatest stress, they do not become values of great magnitude that can have a considerable negative impact on the drone.

III. Results

A. *Drone Stability Analysis*

For stability, as obtained in Fig. 7, it is set for an angle of attack of 4°. It should be noted that this value refers to the inclination as a whole (wing, fuselage, tail, etc.). Otherwise, as shown in Table I, it is the individual base inclination with respect to a set tilt angle of 0° (starting position of the drone).

TABLE I
MAIN CONFIGURATION TABLE FOR STABILITY

Main Configuration	Section		
	Wing	Elevator	Rudder
NACA	3412, 4412	0012	0012
S (m2)	0.32	0.04	0.01
AoA[a] (°)	2	-3.5	N.P[b]

[a]Angle of attack [b]Does not present

In this way, with the wing configuration defined, a stability simulation is carried out in the Xflr5 software against different angles of attack (AoA) as shown below:

Fig. 21. Stability simulation with 0° of angle of attack in Xflr5

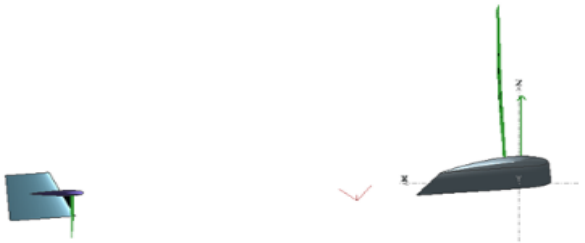

Fig. 22. Stability simulation with 4° of angle of attack in Xflr5

Fig. 23. Stability simulation with 8° of angle of attack in Xflr5

It is observed that for an angle of attack less than and greater than 4°, the generated moments maintain an opposite direction in order to generate a self-inclination towards the stable value.

B. Structural Analysis of the Drone

What can be seen in Table II is that for the static analysis carried out in Inventor, there are considerably high values for both deformation and Von Mise stress. When interpreting these, it should be borne in mind that the analyses have been carried out with loads greater than those that the drone will be affected; under normal conditions, with a load of 100N, the maximum deformation would be 18.12mm, while the Von Mises stress would be only 122.8MPa in just one section of the supports.

TABLE II
STATIC-DYNAMIC ANALYSIS RESULTS TABLE

Analysis Table	Static (Inventor)		Dynamic (Ansys)	
	Min	Max	Min	Max
Deformation (mm)	0	45.29	0	1.543e-2
VM[a] Stress (MPa)	0	307.1	7.3e-7	1.655e-2

[a]Von Mises Stress

IV. CONCLUSIONS

It was concluded that the definition and selection of a NACA wing profile guarantees a functional design and excellent results. This process is a priority since, seen in flight theory, the wing profile generates the lifting forces.

The use of Xflr5 software was of crucial importance for the development of a preliminary prototype, to be able to perform analyses and define mechanical design parameters. Likewise, other simulation and design software guarantee the solidity of the structure when subjected to the normal efforts of the drone's tasks.

In the design of the drone, for cruising speed, the presence of self-stability is important. Which was defined, for this study, in an angle of attack of 4°. This parameter validates that the drone in the face of different planned and unforeseen disturbances self-stabilizes without the need for a control system and / or human intervention.

It is observed that even exposing the model to great efforts, simulating extreme situations where the support in theory doubles the weight, the design responds with a certain tolerance and allows to maintain the solid structure.

For a speed of 30m/s, chosen for design, the model is not only stable but also presents tiny deformation and stress values, imperceptible for any effect.

V. ACKNOWLEDGMENTS

To the Research Directorate of the Peruvian University of Applied Sciences for the support provided to carry out this research work UPC-EXPOST-2022-2

REFERENCES

[1] La República. (2020). Bancos de sangre en rojo. Recuperado 11 de abril de 2021, de https://larepublica.pe/domingo/2020/07/05/bancos-de-sangre-en-rojo/?ref=lre

[2] OMS. (2017). 10 datos sobre las transfusiones de sangre. Recuperado 11 de abril de 2021, de https://www.who.int/features/factfiles/blood_transfusion/es/

[3] Zipline. (2021). Vital, On-Demand Delivery for the World. Recuperado 19 de abril de 2021, de https://flyzipline.com/

[4] Bobela, S. (2018). Final Project Thesis. Aalborg University.

[5] Ling, G., & Draghic, N. (2019). Aerial drones for blood delivery. Transfusion, 59(S2), 1608-1611. https://doi.org/10.1111/trf.15195

[6] Esteban Roncero S. (2011). Introducción a los Perfiles NACA. Recuperado 9 de mayo de 2021, de http://www.aero.us.es/adesign/Slides/Extra/Aerodynamics/Tema_05.1_Extra_Introducci%C3%B3n_Perfiles_NACA.pdf

[7] Wankmüller, C., Kunovjanek, M., Mayrgündter, S. (2021). Drones in emergency response – evidence from cross-border, multi-disciplinary usability tests. International Journal of Disaster Risk Reduction. doi.org/10.1016/j.ijdrr.2021.102567

[8] Kucharczyk, M., Hugenholtz, C. (2021). Remote sensing of natural hazard-related disasters with small drones: Global trends, biases, and research opportunities. Kucharczyk, M., Hugenholtz, C. (2021). Remote sensing of natural hazard-related disasters with small drones: Global trends, biases, and research opportunities. doi.org/10.1016/j.rse.2021.112577

[9] Lakshman, S., Ebenezer, D. (2021). Integration of internet of things and drones and its future applications. Materials Today: Proceedings. doi.org/10.1016/j.matpr.2021.05.039

[10] Dukkanci, O., Kara, B., Bektaş, T. (2021). Minimizing energy and cost in range-limited drone deliveries with speed optimization. Transportation Research Part C:

Emerging Technologies. doi.org/10.1016/j.trc.2021.102985

[11] Moshref-Javadia, M., Winkenbach, M. (2021). Applications and Research avenues for drone-based models in logistics: A classification and review. Expert Systems with Applications. doi.org/10.1016/j.eswa.2021.114854

[12] Chen, X., Ulmer, M., Thomas, M. (2021). Deep Q-learning for same-day delivery with vehicles and drones. European Journal of Operational Research. doi.org/10.1016/j.ejor.2021.06.021

[13] Moshref-Javadia, M., Hemmati, A., Winkenbach, M. (2021). A comparative analysis of synchronized truck-and-drone delivery models. Computers & Industrial Engineering. doi.org/10.1016/j.cie.2021.107648

[14] Burke, C., Nguyen, H., Magilligan, M., & Noorani, R. (2019). Study of A Drone's Payload Delivery Capabilities Utilizing Rotational Movement. 2019 International Conference on Robotics,Electrical and Signal Processing Techniques (ICREST). doi:10.1109/icrest.2019.8644318

[15] Sanjana, P., & Prathilothamai, M. (2020). Drone Design for First Aid Kit Delivery in Emergency Situation. 2020 6th International Conference on Advanced Computing and Communication Systems (ICACCS). doi:10.1109/icaccs48705.2020.907448.

[16] D. Cáceres, M. Dominguez, L. Vinces and J. Ronceros, "Design of a parabolic solar collector for the drying of Spirulina and Cushuro microalgae," 2021 IEEE XXVIII International Conference on Electronics, Electrical Engineering and Computing (INTERCON), 2021, pp. 1-4, doi: 10.1109/INTERCON52678.2021.9532981.

[17] C. Padilla, A. Vivanco, L. Vinces and M. Klusmann, "Design of a multi-hole cylindrical extruder, driven by a linear actuator and used for the formation of bakery dough," 2020 IEEE XXVII International Conference on Electronics, Electrical Engineering and Computing (INTERCON), 2020, pp. 1-4, doi: 10.1109/INTERCON50315.2020.9220251.

[18] G. A. Paredes Farfan, F. Moises Neira Verastegui, L. N. Vinces Ramos and J. Fortunato Oliden Martínez, "Design of a system for the external washing and winding of fire hoses composed of a polyester and rubber jacket," 2020 IEEE XXVII International Conference on Electronics, Electrical Engineering and Computing (INTERCON), 2020, pp. 1-4, doi: 10.1109/INTERCON50315.2020.9220188.

[19] Robledo, A.F., Gambini, P., Vinces, L., Klusmann, M. (2022). A Design of a Spindle and Mathematical Calculations of the Speed Required for HDPE Plastic Extrusion and Recycled PETG Plastic to Obtain 40 kg/h of Filaments 3 mm Thick. In: Iano, Y., Saotome, O., Kemper Vásquez, G.L., Cotrim Pezzuto, C., Arthur, R., Gomes de Oliveira, G. (eds) Proceedings of the 7th Brazilian Technology Symposium (BTSym'21). BTSym 2021. Smart Innovation, Systems and Technologies, vol 295. Springer, Cham. https://doi.org/10.1007/978-3-031-08545-1_50

[20] Loayza, J.C., Ronceros, J., Vinces, L. (2022). A Thermal Analysis of the Internal Flow in 2 Helical Coils for the Delignification Process of Sugar Cane Bagasse Using Superheated Steam. In: Iano, Y., Saotome, O., Kemper Vásquez, G.L., Cotrim Pezzuto, C., Arthur, R., Gomes de Oliveira, G. (eds) Proceedings of the 7th Brazilian Technology Symposium (BTSym'21). BTSym 2021. Smart Innovation, Systems and Technologies, vol 295. Springer, Cham. https://doi.org/10.1007/978-3-031-08545-1_44

[21] del Riego, D.G., Gómez, G., Vinces, L. (2022). An Optimal Blade Design for Mini Wind Generators Mountable on the Spoiler of a Vehicle. In: Iano, Y., Saotome, O., Kemper Vásquez, G.L., Cotrim Pezzuto, C., Arthur, R., Gomes de Oliveira, G. (eds) Proceedings of the 7th Brazilian Technology Symposium (BTSym'21). BTSym 2021. Smart Innovation, Systems and Technologies, vol 295. Springer, Cham. https://doi.org/10.1007/978-3-031-08545-1_52

[22] Tocón, A., Vásquez, C., Vinces, L. (2022). Design of a Hydrodynamic Profile for an Unmanned Underwater Device Using Numerical Simulation. In: Iano, Y., Saotome, O., Kemper Vásquez, G.L., Cotrim Pezzuto, C., Arthur, R., Gomes de Oliveira, G. (eds) Proceedings of the 7th Brazilian Technology Symposium (BTSym'21). BTSym 2021. Smart Innovation, Systems and Technologies, vol 295. Springer, Cham. https://doi.org/10.1007/978-3-031-08545-1_47

[23] Mulatillo, A., Sernaque, C., Ronceros, J., Vinces, L. (2022). Simulation of a System for Reducing Gases Emitted in a Steel Casting Process by Two-Stage Centrifugal Separation. In: Iano, Y., Saotome, O., Kemper Vásquez, G.L., Cotrim Pezzuto, C., Arthur, R., Gomes de Oliveira, G. (eds) Proceedings of the 7th Brazilian Technology Symposium (BTSym'21). BTSym 2021. Smart Innovation, Systems and Technologies, vol 295. Springer, Cham. https://doi.org/10.1007/978-3-031-08545-1_51

[24] J. Uyejara, S. Jurado and L. Vinces, "A numerical simulation of track shoe traction with varying geometrical parameters in low friction coefficient soils," 2022 Congreso Internacional de Innovación y Tendencias en Ingeniería (CONIITI), 2022, pp. 1-5, doi: 10.1109/CONIITI57704.2022.9953639.

[25] G. Vilcamiza, N. Trelles, L. Vinces and J. Oliden, "A coffee bean classifier system by roast quality using convolutional neural networks and computer vision implemented in an NVIDIA Jetson Nano," 2022 Congreso Internacional de Innovación y Tendencias en Ingeniería (CONIITI), Bogota, Colombia, 2022, pp. 1-6, doi: 10.1109/CONIITI57704.2022.9953636.

[26] J. A. Casas, J. Chavez, J. Oliden and L. Vinces, "Numerical simulation of a greenhouse coffee drying system using a continuous flow of hot air," 2022 IEEE ANDESCON, Barranquilla, Colombia, 2022, pp. 1-6, doi: 10.1109/ANDESCON56260.2022.9989935.

[27] L. Auris, M. Gallegos, L. Vinces and J. Ronceros, "A soft grip design using Finite Element Analysis for mango handling on the KUKA KR3 robot," 2022 IEEE ANDESCON, Barranquilla, Colombia, 2022, pp. 1-5, doi: 10.1109/ANDESCON56260.2022.9989799.

[28] L. Tirado, L. Vinces and J. Ronceros, "An interface based on QgroundControl for the rapid parameterization of flights from an embedded system for the control of an inspection drone," 2022 Congreso Internacional de Innovación y Tendencias en Ingeniería (CONIITI), Bogota, Colombia, 2022, pp. 1-5, doi: 10.1109/CONIITI57704.2022.9953724.

[29] A. Rojas, L. Vinces and J. Ronceros, "A numerical simulation of the mechanical structure of an ankle exoskeleton oriented to elderly people," 2022 IEEE ANDESCON, Barranquilla, Colombia, 2022, pp. 1-6, doi: 10.1109/ANDESCON56260.2022.9989639.